Electrical properties of modulation-doped rf-sputtered polycrystalline MgZnO/ZnO heterostructures

2011 J. Phys. D: Appl. Phys. 44 455101

(http://iopscience.iop.org/0022-3727/44/45/455101)

J. Phys. D: Appl. Phys. **44** (2011) 455101 (4pp) doi:10.1088/0022-3727/44/45/455101

Electrical properties of modulation-doped rf-sputtered polycrystalline MgZnO/ZnO heterostructures

H-A Chin[1], I-C Cheng[1,4], C-K Li[1], Y-R Wu[1], J Z Chen[2], W-S Lu[3] and W-L Lee[3]

[1] Graduate Institute of Photonics and Optoelectronics and Department of Electrical Engineering, National Taiwan University, Taipei 10617, Taiwan
[2] Institute of Applied Mechanics, National Taiwan University, Taipei 10617, Taiwan
[3] Institute of Physics, Academia Sinica, Taipei 11529, Taiwan

E-mail: ichuncheng@cc.ee.ntu.edu.tw

Received 15 August 2011, in final form 4 October 2011
Published 28 October 2011
Online at stacks.iop.org/JPhysD/44/455101

Abstract
Modulation doping effect is studied in large-area rf-sputtered polycrystalline MgZnO/ZnO heterostructures. Both polarization effect at the MgZnO/ZnO interface and carrier transferring from the modulation doping layer contribute to the improvement of electrical conductivity of the heterostructure. Modulation doping provides greater enhancement in electrical properties when Mg content in the barrier layer is lower. Temperature-independent carrier concentration is observed in low-temperature Hall measurement, indicating the existence of two-dimensional electron gas in the modulation-doped polycrystalline MgZnO/ZnO structure. The slight drop in mobility at low temperatures is caused mainly by the roughness scattering and impurity scattering.

(Some figures may appear in colour only in the online journal)

1. Introduction

Zinc oxide (ZnO) has shown great potential in electronic and optoelectronic applications [1–5]. Similar to AlGaN/GaN heterostructures, high-quality ZnO along with MgZnO has been implemented to demonstrate two-dimensional electron gas (2DEG) with the advantages of high saturation velocity and low lattice mismatch [6–11]. MgZnO/ZnO systems are therefore promising in high electron mobility transistor (HEMT) applications [12–14]. However, obtaining MgZnO and ZnO of high quality often requires techniques of molecular beam epitaxy and pulse laser deposition, which are not compatible with low-cost large-area electronic and optoelectronic technology. Nevertheless, our previous studies show that even in a defective rf-sputtered polycrystalline MgZnO/ZnO heterostructure the enhancement in electrical properties remains, which is attributed to the screening of defects and grain boundary potential by a large number of carriers induced by the polarization effect [15, 16]. In addition to 2DEG induced by the polarization effects, modulation doping has been proposed to enhance the electrical properties in MgZnO/ZnO heterostructures of high-quality crystals [17]. For a defective polycrystalline MgZnO/ZnO system, similar enhancement has been demonstrated by numerical simulation [16]. This paper reports the experimental evidence.

2. Experiment

A ∼150 nm ZnO thin film was first deposited on Corning Eagle-2000 glass at room temperature by rf sputtering, followed by post-annealing at 600 °C for 30 min to reinforce grain formation. Then a 10/100 nm titanium/gold bilayer was deposited by e-beam evaporation and patterned as coplanar electrical contacts. Next, layers of ∼0.75 nm $Mg_zZn_{1-z}O$, ∼5 nm $Mg_{x-0.025}Zn_{1-x-0.025}O:Al_{0.05}$ and ∼20 nm $Mg_zZn_{1-z}O$ were consecutively rf-sputtered at room temperature upon the patterned electrodes to form the modulation doping structure, as shown in figure 1(*a*). The thicknesses of the MgZnO layers were estimated by the

[4] Author to whom any correspondence should be addressed. Present address: No. 1, Sec. 4, Roosevelt Rd., Taipei 10617, Taiwan.

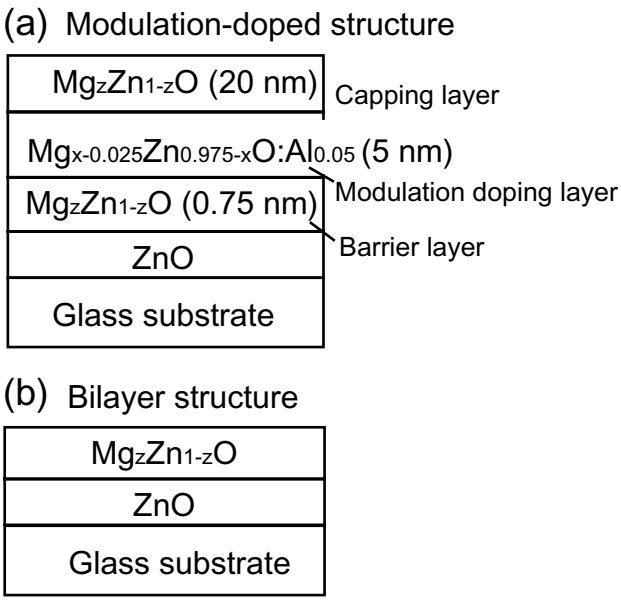

Figure 1. Schematics of (*a*) the modulation-doped structure and (*b*) the bilayer structure. The thickness of the $Mg_zZn_{1-z}O$ layer in the bilayer structure is the saturation thickness indicated in [15].

average deposition rate. The first $Mg_zZn_{1-z}O$ thin layer is the barrier layer, which allows the carriers to transfer from the $Mg_{x-0.025}Zn_{1-x-0.025}O:Al_{0.05}$ modulation doping layer to the $Mg_zZn_{1-z}O$/ZnO interface, while the second $Mg_zZn_{1-z}O$ layer is the capping layer, which pins the Fermi level of the heterostructure for higher transferring possibility. A bilayer heterostructure composed of a thin $Mg_zZn_{1-z}O$ capping layer deposited on top of the ZnO thin film [15], as illustrated in figure 1(*b*), was fabricated for comparison. The electrical characteristics of the heterostructures were evaluated by both coplanar two-point current–voltage measurement and Hall measurement with van der Pauw geometry. The deposition conditions for the ZnO, $Mg_zZn_{1-z}O$, $Mg_{x-0.025}Zn_{1-x-0.025}O:Al_{0.05}$ layers were as follows: oxygen to argon mass flow ratio of 1/6, 1/6 and 0, respectively, rf power density of 2.2 W cm^{-2} and processing pressure of 10 mTorr. Although the as-deposited ZnO exhibits certain crystallinity, post-annealing remains necessary for the observation of conductance enhancement by the presence of 2DEG [15]. The Hall mobility and background sheet carrier concentration in the annealed polycrystalline ZnO thin film are ~1.46 cm^2 V^{-1} s^{-1} and ~5.69 × 10^{12} cm^{-2}, respectively.

3. Results and discussion

3.1. Mg effect in the modulation doping layer

To study the effect of Mg content in the modulation doping layer on the electrical properties of the resulting heterostructure, x in $Mg_{x-0.025}Zn_{1-x-0.025}O:Al_{0.05}$ is varied from 15% to 40% while the compositions of barrier and capping layers are fixed at $Mg_{0.15}Zn_{0.85}O$. Figure 2 shows that as x increases, the sheet resistance of the heterostructure decreases and the sheet carrier density increases. The possible reason for the increase in carrier density is that when the

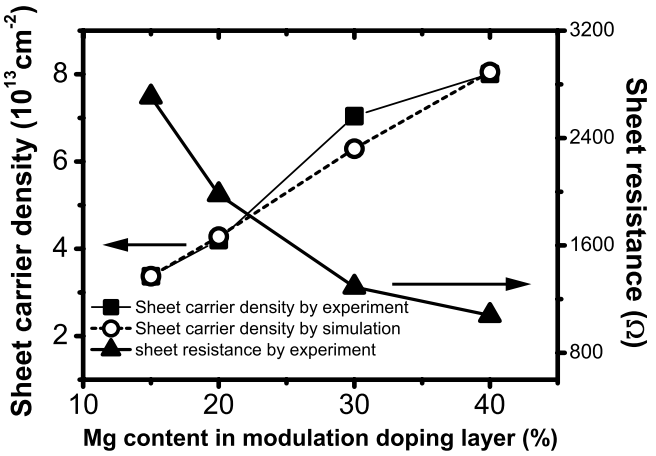

Figure 2. Sheet carrier density and sheet resistance of the heterostructure with modulation doping layer of different Mg content. The barrier and capping layers are $Mg_{0.15}Zn_{0.85}O$ and the modulation doping layer is $Mg_{x-0.025}Zn_{0.975-x}O:Al_{0.05}$ with x = 15%, 20%, 30% and 40%. The closed symbols represent the experimental results, while the open symbols are the simulation results. The lines are drawn as a guide to the eye.

Mg content is raised, the band gap of MgZnO : Al increases [18, 19] and the energy difference between the donor level in the MgZnO : Al layer and the conduction band edge of ZnO at the $Mg_zZn_{1-z}O$/ZnO interface becomes larger, which makes the carriers have greater tendency to transfer from the $Mg_{x-0.025}Zn_{0.975-x}O:Al_{0.05}$ modulation doping layer into the $Mg_zZn_{1-z}O$/ZnO interface, i.e. the 2DEG region. Therefore, with x = 0.4 in the modulation doping layer, the resulting heterostructure reveals the lowest sheet resistance. In addition, if the carrier concentration in the modulation doping layer is higher than a critical value, the Fermi level of the modulation doping layer would rise above the conduction band edge and the carriers tend to remain in the modulation doping layer rather than transferring into the 2DEG confinement region, as indicated in previous simulation results [16, 17].

The experimental result in figure 2 is further studied using 1D Poisson and Schrödinger solver for the sheet carrier density and the distribution in the heterostructure. The simulation parameters used are the ratio of conduction and valence band offsets of 6/4 [20, 21], polarization charge density of 2.5 × 10^{13} cm^{-2} at the $Mg_{0.15}Zn_{0.85}O$/ZnO interface, which was extracted from the sheet carrier concentrations of the bilayer heterostructure as shown in figure 3, and an activation energy of 130 meV for carriers in the $Mg_{x-0.025}Zn_{0.975-x}O:Al_{0.05}$ modulation doping layer. Based on the experimental results shown in figure 2, the doping level of the $Mg_{x-0.025}Zn_{0.975-x}O:Al_{0.05}$ modulation doping layer was fitted to be 3 × 10^{20} cm^{-3}. The simulation result reveals that ~35%, ~44%, ~55% and ~61% of the carriers in the heterostructures are contributed by the activated $Mg_{x-0.025}Zn_{0.975-x}O:Al_{0.05}$ modulation doping layer for x = 0.15, 0.2, 0.3 and 0.4, respectively.

3.2. Mg effect in barrier and capping layers

To study the effect of Mg content in the overlying barrier and capping layers on the electrical properties of the resulting

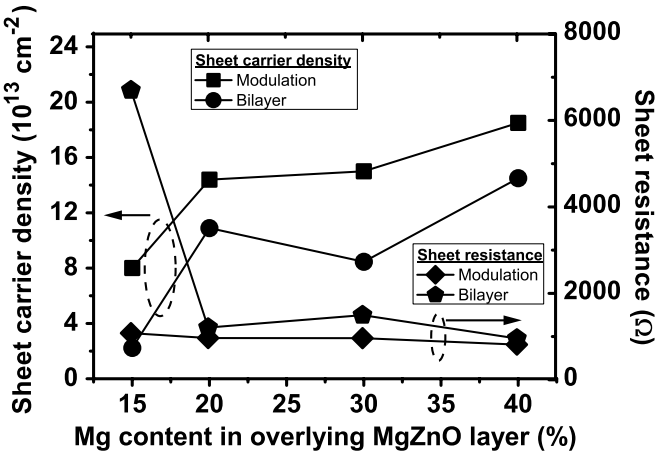

Figure 3. Sheet resistances and sheet carrier densities of the modulation-doped heterostructure and its counterpart, the bilayer heterostructure.

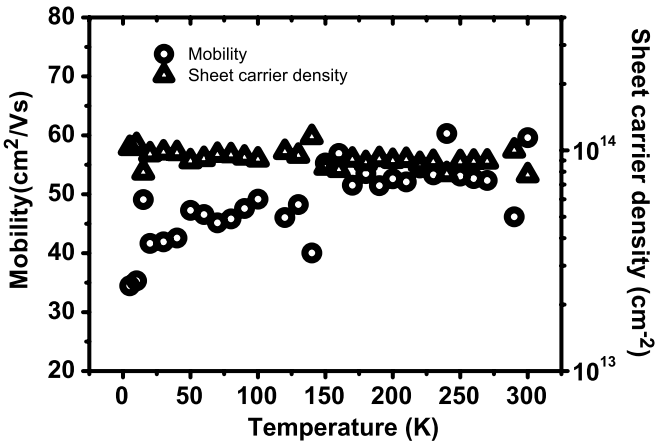

Figure 4. Hall mobility and sheet carrier density of the modulation-doped heterostructure as a function of temperature. The composition of the barrier and capping layers is $Mg_{0.15}Zn_{0.85}O$, and the composition of the modulation doping layer is $Mg_{0.375}Zn_{0.575}O : Al_{0.05}$.

heterostructure, z in $Mg_zZn_{1-z}O$ is varied from 15% to 40% while the composition of the modulation doping layer is fixed at an Mg content of 40% and Al content of 5%. Figure 3 shows the sheet carrier densities and sheet resistances of the modulation-doped heterostructure and its counterpart, the bilayer heterostructure, versus Mg content in the overlying $Mg_zZn_{1-z}O$ layer(s). As the Mg content in the barrier layer increases, the resulting sheet resistance decreases despite the large band gap of the barrier layer. However, most significant improvement of the electrical properties is observed in the modulation-doped heterostructure with an Mg content of 15% in the overlying $Mg_zZn_{1-z}O$ layers in comparison with its counterpart, the bilayer heterostructure. The improvement becomes negligible as the Mg content increases. This indicates that at a low Mg content the carrier transferring from the modulation doping layer can significantly contribute to the electrical conductivity and carrier concentration, while at a high Mg content the large band gap of the barrier layer reduces the carrier transferring probability but the electrical properties are compensated by the large polarization effect.

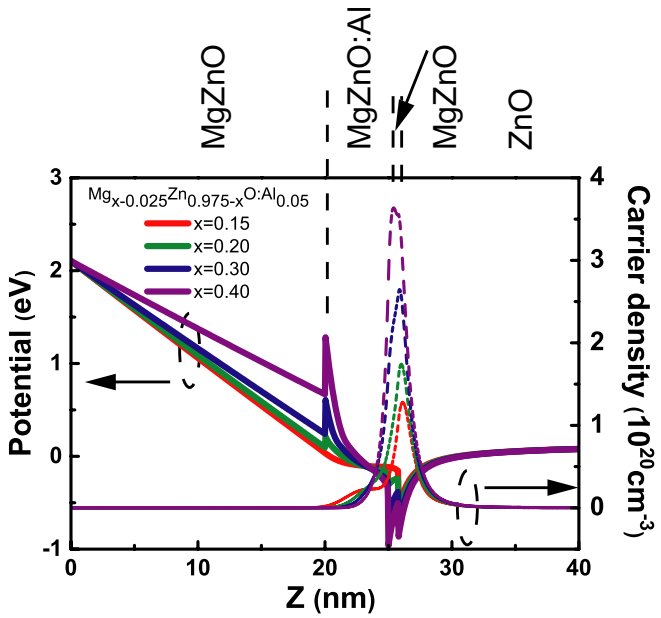

Figure 5. Simulation results for carrier and potential distributions in the heterostructure with a modulation doping layer of different Mg content. The composition of the barrier and capping layers is $Mg_{0.15}Zn_{0.85}O$ and the composition of the modulation doping layer is $Mg_{x-0.025}Zn_{0.975-x}O : Al_{0.05}$ with $x = 15\%$, 20%, 30% and 40%.

3.3. Carrier density and mobility

Figure 4 shows the sheet carrier density and mobility for the modulation-doped heterostructure obtained by low-temperature Hall measurements. The sheet carrier density remains nearly constant throughout the whole temperature range, indicating that the carrier is 2DEG and not thermally activated. Merely a slight decrease in mobility at low temperatures indicates the dominant scattering mechanism is roughness scattering together with minor impurity and alloy scattering [22–24]. The simulation result shown in figure 5 indicates that the carrier distribution shift towards the modulation doping layer slightly as the Mg content in the modulation doping layer increases. Therefore, the slight decrease in mobility at low temperatures is attributed to the impurity scattering and alloy scattering from the modulation doping layer.

4. Conclusion

We have shown that a modulation doping layer can increase the carrier concentration in an rf-sputtered polycrystalline MgZnO/ZnO heterostructure. The sheet carrier concentration increases with increasing Mg content in the MgZnO : Al modulation doping layer. The nearly constant sheet carrier concentration observed in the low-temperature Hall measurement confirms the existence of 2DEG in the modulation-doped polycrystalline MgZnO/ZnO structure. The slight drop in mobility at low temperatures shows the modulation doping scheme successfully increases the carrier concentration while mitigating the impurity scattering in this rf-sputtered heterostructure.

Acknowledgments

The authors would like to thank the Material and Chemical Research Laboratories, Industrial Technology Research Institute for the early financial and technical support. ICC and JZC gratefully acknowledge the funding support from the National Science Council of Taiwan ROC, under Grant Nos NSC 100-2221-E-002-151-MY3, NSC 100-3113-E-002-012 (ICC) and NSC 100-2627-M-002-002 (JZC).

References

[1] Cong C X, Yao B, Zhou Q J and Chen J R 2008 *J. Phys. D: Appl. Phys.* **41** 105303
[2] Choi C H and Kim S H 2005 *J. Cryst. Growth* **283** 170
[3] Hiramatsu M, Imaeda K, Horio N and Nawata M 1998 *J. Vac. Sci. Technol.* A **16** 669
[4] Nakano M, Tsukazaki A, Ohtomo A, Ueno K, Akasaka S, Yuji H, Nakahara K, Fukumura T and Kawasaki M 2010 *Adv. Mater.* **22** 876
[5] Jeong J A, Shin H S, Choi K H and Kim H K 2010 *J. Phys. D: Appl. Phys.* **43** 465403
[6] Tampo H, Shibata H, Matsubara K, Yamada A, Fons P and Niki S 2006 *Appl. Phys. Lett.* **89** 132113
[7] Edahiro T, Fujimura N and Ito T 2003 *J. Appl. Phys.* **93** 7673
[8] Brandt M, von Wenckstern H, Benndorf G, Hochmuth H, Lorenz M and Grundmann M 2009 *Thin Solid Films* **518** 1048
[9] Tsukazaki A, Akasaka S, Nakahara K, Ohno Y, Ohno H, Maryenko D, Ohtomo A and Kawasaki M 2010 *Nature Mater.* **9** 889
[10] Ohtomo A, Kawasaki M, Koida T, Masubuchi K, Koinuma H, Sakurai Y, Yoshida Y, Yasuda T and Segawa Y 1998 *Appl. Phys. Lett.* **72** 2466
[11] Westmeyer A N, Mahajan S, Bajaj K K, Lin J Y, Jiang H X, Koleske D D and Senger R T 2006 *J. Appl. Phys.* **99** 013705
[12] Koike K, Nakashima I, Hashimoto K, Sasa S, Inoue M and Yano M 2005 *Appl. Phys. Lett.* **87** 112106
[13] Sasa S, Ozaki M, Koike K, Yano M and Inoue M 2006 *Appl. Phys. Lett.* **89** 053502
[14] Sasa S, Hayafuji T, Kawasaki M, Koike K, Yano M and Inoue M 2007 *IEEE Electron Device Lett.* **28** 543
[15] Chin H A, Cheng I C, Huang C I, Wu Y R, Lu W S, Lee W L, Chen J Z, Chiu K C and Lin T S 2010 *J. Appl. Phys.* **108** 054503
[16] Huang C I, Chin H A, Wu Y R, Cheng I C, Chen J Z, Chiu K C and Lin T S 2010 *IEEE Trans. Electron Devices* **57** 696
[17] Cohen D J and Barnett S A 2005 *J. Appl. Phys.* **98** 053705
[18] Lu J G, Fujita S, Kawaharamura T, Nishinaka H, Kamada Y and Ohshima T 2006 *Appl. Phys. Lett.* **89** 262107
[19] Matsubara K, Tampo H, Shibata H, Yamada A, Fons P, Iwata K and Niki S 2004 *Appl. Phys. Lett.* **85** 1374
[20] Coli G and Bajaj K K 2001 *Appl. Phys. Lett.* **78** 2861
[21] Su S C, Lu Y M, Zhang Z Z, Shan C X, Li B H, Shen D Z, Yao B, Zhang J Y, Zhao D X and Fan X W 2008 *Appl. Phys. Lett.* **93** 082108
[22] Singh J 1993 *Physics of Semiconductors and their Heterostructures* (New York: McGraw-Hill) pp 357–96
[23] Gold A 2010 *Appl. Phys. Lett.* **96** 242111
[24] Thongnum A, Sa-yakanit V and Pinsook U 2011 *J. Phys. D: Appl. Phys.* **44** 325109